Novel Design Strategy of Multiple-Resonance-Type Blue Fluorescent Dopants with High Efficiency and High Color Purity

Dayeon Lee[1], *Jangho Moon*[2], *Jun Yeob Lee*[1,2*]

[1]School of Chemical Engineering, Sungkyunkwan University, 2066, Seobu-ro, Jangan-gu, Suwon-si, Gyeonggi-do, 16419, Republic of Korea

[2]Department of Display Convergence Engineering, Sungkyunkwan University, 2066, Seobu-ro, Jangan-gu, Suwon-si, Gyeong-gi-do, 16419, Republic of Korea

E-mail : leej17@skku.edu

Abstract

Deep blue boron based multiple resonance (MR) type fluorescent materials, BD-1 and BD-2 were synthesized and evaluated. Benzo[b]thiophene substituent which has low triplet energy was introduced to lower triplet energy to suppress the intermolecular interactions. Furthermore, bulky donating group was introduced to control the wavelength, color purity, and to increase molecular distance. As a result, BD-2 based fluorescent device showed CIE coordinates of (0.134,0.087) and EQE$_{max}$ of 7.9%.

Keywords

Keywords: blue OLEDs·multiple resonance·fluorescence· high color purity·high efficiency

1. Objective and Background

On account of high luminous energy of blue emitters, electrical stress applied to the materials during operating OLED device is unavoidable. This electrical stress could degradate organic materials and cause serious decrease in device life time.(1, 2) Due to low efficiency of blue fluorescent materials, research on thermally activated delayed fluorescence (TADF) and phosphorescent dopants has been actively conducted. However, short device lifetime and poor color purity make it difficult to practically apply TADF and phosphorescent dopants in the industry. In that reason, blue fluorescent materials are still preferred over materials utilizing other emission mechanisms in terms of stability and efficiency.(3)

As blue fluorescence emitters, anthracene and pyrene-based materials have been widely studied. However, these polycyclic aromatic compounds have large Stokes shift, large full width at half maximum (FWHM) and low external quantum efficiency (EQE). Among these several disadvantages of conventional fluorescent dopants, poor color purity, gained from their strong vibrational peak makes it much difficult to realize ultra-high-resolution display.(4) To overcome the issue of poor color purity of conventional fluorescent emitters, various blue fluorescent materials with narrow FWHM have been developed. However, challenges such as reduced device lifetimes or low efficiency have emerged due to the involvement of triplet excitons in the emission mechanism through delayed fluorescence properties.(5)

Meanwhile, Hatakeyama group reported a boron-based multiple resonance (MR)-type TADF materials.(6) The alternating short-range orbital distributions at the atomic scale of MR materials result in excellent color purity, with a small Stokes shift and narrow FWHM, exceeding the performance of conventional fluorescent materials. Additionally, due to the high overlap between the highest occupied moleculr orbital (HOMO) and lowest unoccupied molecular orbital (LUMO), these materials exhibit a fast radiative decay rate and high luminous efficiency. However, MR-TADF emitters tend to have long-lived triplet excitons, which may result in significant chemical degradation processes initiated in the triplet state. Furthermore, the rigid and planar core structure of these materials can cause concentration quenching effects at high doping concentrations.(7,8) To overcome these drawbacks and enhance the longevity and color purity of OLED devices, it is crucial to develop emitters that do not undergo delayed fluorescence and to provide proper blocking groups that could create chemical spaces between EML molecules, thereby suppressing Dexter energy transfer and concentration quenching effect.(9,10)

In this study, we synthesized and evaluated two boron-based MR-type blue emitters as fluorescent dopant. In order to prevent TADF mechanism of fluorescent emitters, a benzo[b]thiophene substituent which has low triplet energy was introduced into the reference material, '2,12-di-tert-butyl-5,9-bis(4-(tert-butyl)phenyl)-5,9-dihydro-5,9-diaza-13b-boranaphtho[3,2,1-de]anthracene' (t-DABNA) to enlarge the energy gap between the singlet (S_1) and triplet (T_1) states. Additionally, t-butyl group was introduced as a blocking group. First compound was named as '2,11-di-tert-butyl-5,9-bis(4-(tert-butyl)phenyl)-5H,9H-14-thia-5,9-diaza-14b-borafluoreno[3,2,1-de]anthracene'(BD-1). A weak, but bulky donor moiety was further introduced at boron-para position of DABNA core to control the wavelength and FWHM of the emitter. This compound was named as BD-2. By introducing weak donor group at the boron-para position, we could realize deep blue emission with narrow FWHM. Also this donor moiety creates a large dihedral angle between the DABNA core and functions as a blocking group, effectively suppresses intermolecular interactions and concentration quenching effects.

2. Results

The density functional theory (DFT) calculation was performed for the newly synthesized MR-type fluorescent materials. DFT and time-dependent DFT (TD-DFT) were calculated using the B3LYP/6-31G basis set, and the frontier molecular orbital (FMO) distribution of the material was shown. The electron distribution of HOMO and LUMO of the core is alternately distributed between electron deficient boron atom and electron rich nitrogen atom as shown in MR-type materials. The introduction of weak electron-donating moiety could increase the electron density around the boron atom, resulting in a shift of the HOMO electron distribution toward the donating group. This electron donation is expected to

ISSN 0097-996X/25/5603-2279-$1.00 © 2025

enhance electron transfer efficiency, thereby improving overall device performance. The large orbital overlap centered on the rigid structure would show high photoluminescence quantum yield (PLQY).

Basic photophysical properties of t-DABNA, BD-1 and BD-2 were measured by ultraviolet-visible (UV-vis) absorption and photoluminescence (PL) emission. The results are shown in **Table 1**. UV-vis absorption spectrum was measured in diluted tetrahydrofuran (THF) solution at room temperature. All compounds showed π-π^* transition bands below 400 nm whereas a strong absorbtion peak caused by short-range charge transfer (SRCT) was similarly observed at 400-480 nm which normally appears in MR-type materials.(7) Fluorescence spectra were measured at room temperature in degassed Toluene and phosphorescence spectra were measured in frozen THF at low temperature (77 K) with delay time of 2.0 ms. As a result, fluorescence emission peaks of BD-1 and BD-2 are shown at 442 nm and 418 nm, 442 nm, respectively. From the PL spectra, singlet emission peaks of BD-1 and BD-2 were observed at 456 nm and 453 nm, respectively. Both synthesized materials showed very narrow FWHM of 26 nm and 21 nm in diluted toluene solution. Deep blue emissions were observed along with a narrow FWHM. Also, the Stokes shift was 14 and 11 nm. These results demonstrate that the MR characteristics of the core material, t-DABNA, have been preserved. Singlet and triplet energy estimated from onset values of fluorescence and phosphorescence spectra for BD-1 and BD-2 were 2.71 eV and 2.34 eV, 2.73 eV and 2.30 eV, respectively. Both t-DABNA and the two newly synthesized materials exhibited similar singlet energy levels. However, due to the introduction of the benzo[b]thiophene substituent, the triplet energy of BD-1 and BD-2 was reduced by more than 0.2 eV, resulting in a larger value of $\triangle E_{ST}$ compared to t-DABNA. This indicates that the emission mechanism can be effectively controlled in the desired direction by introducing the appropriate substituent, as intended.

Table 1. Summry of photophysical properties of t-DABNA (Ref.), BD-1 and BD-2

	Abs. (nm)	PL (nm)	FWHM (nm)	Phos. (nm)	E_{S1} (eV)	E_{T1} (eV)	ΔE_{ST} (eV)
t-DABNA	-	457	26.3	489	2.71	2.54	0.17
BD-1	442	456	26	529	2.71	2.34	0.37
BD-2	418, 442	453	21	539	2.73	2.30	0.43

Additional analysis was performed to analyze the time-related emissive properties of MR-type emitters on thin films. Doped films were fabricated with 3 wt% doping concentration of the emitters on the 9-(3- (phenanthren-9-yl)phenyl)-10-phenylanthracene (TTF-Phen), triplet-triplet fusion (TTF) type host. Table 2 shows the results of transient PL and PL quantum yield (PLQY) analysis on the doped film. BD-1 showed the longest prompt component decay time (τ_p) compared to others. Due to its planar geometry of BD-1, π-π stacking of dopant materials may increased compared to other 2 compounds. Increased π-π stacking contributed to intermolecular emissive state showing a slower singlet exciton decay time. On the other hand, BD-2, in which an appropriate blocking group was introduced, resulted in accelerated prompt component decay time (τ_p) of 5.4 ns. No delayed component decay time (τ_d) was observed for both BD-1 and BD-2, which can be interpreted as a changed emission mechanism to fluorescence rather than TADF, reducing effect of high energy triplet components. This result experimentally demonstrated the effectiveness of design strategy of introducing the benzo[b]thiophene substituent.

The absolute PLQY was measured under a nitrogen atmosphere with same doped films. As a result, PLQYs of t-DABNA, BD-1 and BD-2 were measured as 90.1%, 98.6% and 86.8%, respectively. BD-1 showed the highest value of PLQY among the 3 emitters, which could lead to higher EQE in device performance.

Table 2. Summary of TRPL and PLQY data of 3 wt% doped film in matrix of TTF-Phen.

	Φ_{PL} (%)	τ_p (ns)	k_{ISC} (10^5 s^{-1})	k_r (10^8 s^{-1})
t-DABNA	90.1	6.0	16.6	1.51
BD-1	98.6	6.8	2.07	1.46
BD-2	86.8	5.4	24.7	1.62

To evaluate the optoelectronic properties of synthesized materials, TTF device was fabricated. The device structure was as follows: ITO (50 nm)/BCFN: HATCN (40 nm, 30 wt%)/BCFN (10 nm)/oCBP (10 nm)/TTF-Phen:emitter (30 nm, 3 wt%)/SBF-Trz (5 nm)/ZADN (20 nm)/LiF/Al (1.5 nm/200 nm). BCFN stands for N-([1,1'- biphenyl]-4-yl)-9,9-dimethyl-N-(4-(9-phenyl-9H-carbazol-3- yl)phenyl)-9H-fluoren-2-amine, HATCN stands for hexaazatriphenylenehexacarbonitrile, oCBP stands for 2,2'-di(9Hcarbazol-9-yl)-1,1'-biphenyl, SBF-Trz stands for 2-(9,9'-spirobi[fluoren]-4-yl)-4,6-diphenyl-1,3,5-triazine, and ZADN stands for 2-(4-(9,10-di(naphthalen-2-yl)anthracen-2-yl)phenyl)-1-phenyl-1H-benzo[d]imidazole. Device structures of fabricated OLED devices are shown in **Figure 1**.

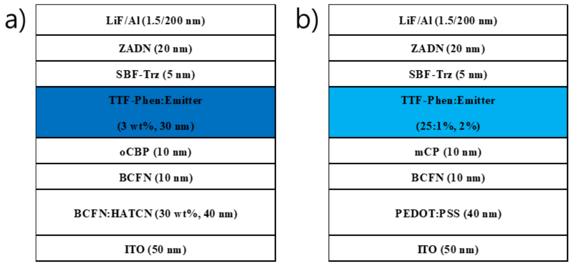

Figure 2. Device structures of TTF device

Device characteristics of TTF devices were illustrated in **Figure 3** and summarized in **Table 2**. BD-1 and BD-2 based devices recorded high external quantum efficiency of 8.0% and 7.9%, respectively. Both devices showed an efficiency roll-off lower than 10% at 1,000 cd/m^2, demonstrating high device stabilities of BD-1 and BD-2. Notably, BD-2 based device showed the narrowest FWHM of 22 nm with suppressed vibrational peak, realizing CIE coordinate of (0.134, 0.084). This result shows a promising design strategy to realize high color purity OLED devices. **Figure 4** shows color coordinates of emitters in TTF type OLEd devices at 100 cd/m^2. Even at 1000 cd/m^2 CIE$_y$ coordinates was not changed a lot, maintain high color purity.

Table 2. Summry of TTF type OLED device.

Device	Voltage (V)	EQE (%)		CIE	λ (nm)	FWHM
	1 cd/m^2	1,000 cd/m^2	Max	100 cd/m^2	100 cd/m^2	100 cd/m^2
t-DABNA	4.0	8.0	8.1	(0.126,0.102)	464	25.8
BD-1	4.2	7.9	8.0	(0.128,0.111)	462	25.6
BD-2	4.4	7.7	7.9	(0.134,0.087)	458	22.8

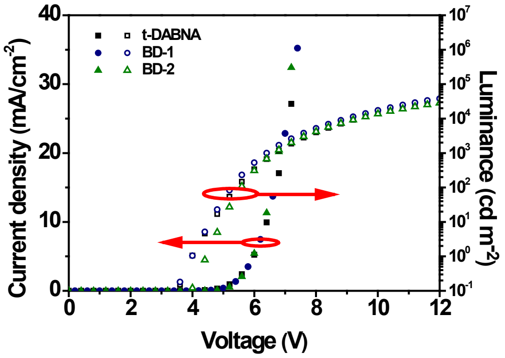

Figure 2. *J-V-L* characteristics of t-DABNA, BD-1 and BD-2 in TTF type OLED device.

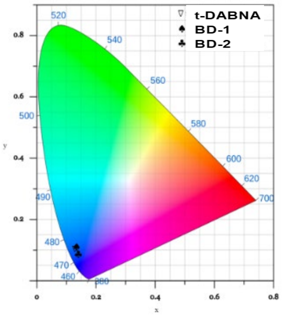

Figure 3. CIE coordinate of t-DABNA, BD-1 and BD-2 in TTF type OLED device

To further evaluate optoelectronic properties of synthesized materials depending on the doping concentration, TTF devices with doping concentration of 1 wt% and 3 wt% was fabricated. The device structure was as follows: ITO (50 nm)/ PEDOT:PSS(40 nm)/BCFN (10 nm)/mCP (10 nm)/TTF-Phen:emitter (25 nm, x wt%)/SBF-Trz (5 nm)/ZADN (20 nm)/LiF/Al (1.5 nm/200 nm). Device structures of fabricated OLED devices are shown in **Figure 2**. Device characteristics of devices were summarized in **Table 3**. EQE$_{max}$ of BD-1 based device with doping concentration of 1wt% and 3wt% were 5.3% and 5.2%, respectively. As the doping concentration increased, decrease of EQE$_{max}$ with slightly red-shifted wavelength of 1 nm and broadened FWHM was observed. The reason for this concentration quenching can be explained through planar molecular structure of BD-1. The planarity of the emitter decreases distance between emitting materials, which leads to activated Dexter energy transfer and accelerated non-radiative decay process, which seriously affects the quantum efficiency of OLED devices. This can be clearly explained through comparison with device properties of BD-2. BD-2 incorporates a bulky blocking group into the BD-1 structure. EQE$_{max}$ of BD-2 based device with doping concentration of 1wt% and 3wt% were 5.6% and 6.1%, respectively. Unlike BD-1, no decrease in efficiency was observed in BD-2, despite the increase in doping concentration, which means introduced blocking moiety effectively suppressed intermolecular interactions and concentration quenching effects. This result demonstrates the importance of introducing proper blocking group to prevent EQE degradation processes of OLED devices. Although BD-2 based devices with doping concentration of 1 wt% and 3wt% showed narrow FWHM of 20.5 nm and 21.5 nm, with CIE coordinates of (0.139, 0.67) and (0.135, 0.083), respectively. BD-2 based device with doping concentration of 1 wt%, showed the narrowest emission bandwidth of 20.5 nm and showed the best color purity. So, it was demonstrated that our new design strategy of blue MR-type fluorescent materials is an effective way to achieve high color purity and long-term device stability.

Table 3. Summry of TTF type OLED device depending on doping concentration.

Device	Voltage (V)	EQE (%)		CIE	λ (nm)	FWHM
	1 cd/m^2	1,000 cd/m^2	Max	100 cd/m^2	100 cd/m^2	100 cd/m^2
BD-1 (1%)	5.2	5.1	5.3	(0.133,0.085)	460	22.9
BD-1 (2%)	5.2	4.9	5.2	(0.131,0.096)	461	23.88
BD-2 (1%)	5.3	5.0	5.6	(0.139,0.067)	456	20.5
BD-2 (2%)	53	5.1	6.1	(0.135,0.083)	458	21.5

3. Impact of Research

The significance of this work is a novel design strategy of developing MR-type blue fluorescence emitter. By controlling energy levels, intermolecular interactions, and HOMO distribution, concentration quenching resistant boron-based MR-type fluorescent emitter was synthesized and characterized. Synthesized materials showed narrow FWHM with deep blue emission with high PLQY. Also, no delayed component decay time (τ_d) was observed for synthesized materials, proving the efficiency of the newly suggested design strategies. BD-1 based TTF-type device showed a high EQE value of 8.0% and narrow FWHM. BD-2 based device showed hardly non-changed EQE variation across different concentrations. The MR characteristics in the core structure delivered a deep blue emission with high color purity and high EQE. Therefore, this work demonstrated promising development of boron-based MR-type fluorescent emitter with high color purity and high efficiency.

4. References

1.Lee J, Chen C, Lee P, Lin H, Leung M, Chiu T, Lin C. Blue organic light-emitting diodes: current status, challenges, and future outlook. Joural of Materials Chemistry C. 2019;7:5874-5888.

2. Monkman A. Why Do We Still Need a Stable Long Lifetime

Deep Blue OLED Emitter?. ACS Appl. Mater. Interfaces. 2021;.

3. Fukagawa H, Shimizu T, Ohbe N, Tokito S, Tokumaru K, Fujikake H. Anthracene derivatives as efficient emitting hosts for blue organic light-emitting diodes utilizing triplet–triplet annihilation. Organic Electronics. 2012;13(7):1197-1203.

4. Hu J, Satoh F, Kawata S, Katagirl H, Sasabe H, Kido J. Bisanthracene-Based Donor–Acceptor-type Light-Emitting Dopants: Highly Efficient Deep-Blue Emission in Organic Light-Emitting Devices. Advanced Functional Materials. 2013;24(14):2064-2071.

5. Hatakeyama T, Shiren K, Nakajima K, Nomura S, Nakatsuka S, Kinoshita K, Ni J, Ono Y, Ikuta T. Ultrapure Blue Thermally Activated Delayed Fluorescence Molecules: Efficient HOMO–LUMO Separation by the Multiple Resonance Effect. Advanced Materials. 2016;28(14):2777-2781.

6. Kim JH, Chung WJ, Kim J, Lee JY. Concentration quenching–resistant multiresonance thermally activated delayed fluorescence emitters. Materialstoday Energy. 2021;21:100792.

7. Suresh SM, Hall D, Beljonne D, Olivier Y, Zysman-Colman E. Multiresonant Thermally Activated Delayed Fluorescence Emitters Based on Heteroatom-Doped Nanographenes: Recent Advances and Prospects for Organic Light-Emitting Diodes. Advanced Functional Materials. 2020;30(33):1908677.

8. Kuma H, Hosokawa C. Blue fluorescent OLED materials and their application for high-performance devices. Scinece and Technology of Advanced Materials. 2014;15(3):034201.

9. Fery C, Racine B, Doyeux H, Cina S. 2005;87:213502. Physical mechanism responsible for the stretched exponential decay behavior of aging organic light-emitting diodes. Applied Physics Letter. 2005;87(21):213502.

10. Lim H, Woo S, Ha YH, Kim Y, Kim J. Breaking the Efficiency Limit of Deep-Blue Fluorescent OLEDs Based on Anthracene Derivatives. Advanced Maerials. 2021.